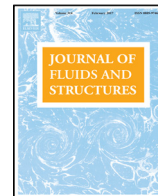




Contents lists available at ScienceDirect

## Journal of Fluids and Structures

journal homepage: [www.elsevier.com/locate/jfs](http://www.elsevier.com/locate/jfs)

# Aeroelastic flutter analysis considering modeling uncertainties

Mikaela Lokatt

KTH Royal Institute of Technology, Aeronautical and Vehicle Engineering, Teknikringen 8, 100 44 Stockholm, Sweden

## HIGHLIGHTS

- A perturbation analysis method for aeroelastic flutter analysis is presented.
- The method allows analysis of both structural and aerodynamic uncertainties.
- The method has favorable computational properties.

## ARTICLE INFO

## Article history:

Received 26 October 2016

Received in revised form 13 June 2017

Accepted 22 June 2017

Available online xxxx

## Keywords:

Flutter analysis

Modeling uncertainty

Generalized eigenproblem

Eigenvalue differential

Minkowski sum

## ABSTRACT

A method for efficient flutter analysis of aeroelastic systems including modeling uncertainties is presented. The aerodynamic model is approximated by a piece-wise continuous rational polynomial function, allowing the flutter equation to be formulated as a set of piece-wise linear eigenproblems. Feasible sets for eigenvalue variations caused by combinations of modeling uncertainties are computed with an approach based on eigenvalue differentials and Minkowski sums. The method allows a general linear formulation for the nominal system model as well as for the uncertainty description and is thus straightforwardly applicable to linearized aeroelastic models including both structural and aerodynamic uncertainties. It has favorable computational properties and, for a wide range of uncertainty descriptions, feasible sets can be computed in output polynomial time. The method is applied to analyze the flutter characteristics of a delta wing model. It is found that both structural and aerodynamic uncertainties can have a considerable effect on the damping trends of the flutter modes and thus need to be accounted for in order to obtain reliable predictions of the flutter characteristics. This indicates that it can be beneficial to allow a flexible and detailed formulation for both aerodynamic and structural uncertainties, as is possible with the present system formulation.

© 2017 Elsevier Ltd. All rights reserved.

## 1. Introduction

Flutter is a dynamic aeroelastic instability in which the interaction of aerodynamic, structural and inertial forces causes the aircraft structure to perform undamped, periodic, oscillations. The structural oscillations can cause problems for the aircraft control system and also damage the aircraft structure. Because of the, sometimes catastrophic, consequences of aircraft flutter, the analysis of flutter instabilities plays an important part in design and flight testing of aircraft (Bisplinghoff and Ashley, 1962; Dowell et al., 2015). During the validation stage, flight testing is used to ensure that the flight envelop is free of flutter instabilities. Both time and money can be saved by using mathematical models, as a complement to experimental testing, to obtain predictions of possible flutter instabilities (Lind and Brenner, 2002; Dowell et al., 2015). This allows flutter

E-mail address: [mlokatt@kth.se](mailto:mlokatt@kth.se).<http://dx.doi.org/10.1016/j.jfluidstructs.2017.06.017>

0889-9746/© 2017 Elsevier Ltd. All rights reserved.

instabilities to be discovered already during the design process and can thus provide information of whether an aircraft needs to be redesigned before its aeroelastic stability is evaluated in flight flutter testing.

It is common to base the mathematical models on linearized, frequency domain, structural and aerodynamic models. The resulting system of equations (nominal system model) forms a non-linear eigenproblem and a number of methods have been developed for its solution (Dowell et al., 2015; Borglund and Eller, 2013). Given accurate structural and aerodynamic models, the mathematical analysis can provide relatively accurate flutter speed predictions. In practice, some deviation between the modeled system dynamics and the actual aircraft dynamics is typically present, which can lead to a, more or less significant, difference between the numerically predicted flutter speed and the flutter speed of the real aircraft.

In order to account for this possible variation, so called robust analysis methods have been developed (Pettit, 2004; Danowsky et al., 2010). Robust analysis methods provide information about flutter speed variations caused by modeling uncertainties. They allow a large number of system variations to be accounted for in one analysis, avoiding the need to perform nominal flutter analyses for all possible combinations of parameter variations which are covered by the uncertainty description. This property is useful in analysis of aeroelastic systems which are subjected to numerous aerodynamic and structural uncertainties, for which a very large number of possible combinations of parameter variations needs to be analyzed.

A common basis for robust analysis is  $\mu$ -analysis, which employs the structured singular value to evaluate the stability of a nominal system model that is subjected to a set of structured uncertainties (Lind and Brenner, 1999). This analysis method originates from the control community and was introduced for aeroelastic analysis by Lind and Brenner (1997) and Lind (2002). Further development of the  $\mu$ -framework for aeroelastic applications was made by Borglund, who developed the  $\mu - k$  method (Borglund, 2004). The  $\mu - k$  method applies  $\mu$ -analysis directly to pre-computed frequency domain matrices and thereby avoids the need to find an approximate state space representation of the aerodynamic forces, as is needed in the classical framework for  $\mu$ -analysis (Lind and Brenner, 1999). In subsequent work Borglund presented the  $\mu - p$  method which not only enables estimation of a lowest (worst case) flutter speed, but also allows computation of feasible sets within which the eigenvalues may vary when the aeroelastic system is subjected to a given set of uncertainties (Borglund, 2008). Computation of feasible sets has shown to provide useful information for validation of uncertainty models (Heinze et al., 2009) as well as for industrial application in flight flutter testing (Leijonhufvud and Karlsson, 2011).

Computing the value of  $\mu$  appears to, in general, be a NP hard problem and thus, in practice, upper and lower bounds of  $\mu$  are computed instead of the exact  $\mu$ -value (Lind and Brenner, 1999). To avoid unnecessarily conservative estimates of the robust flutter boundaries, it is important to find upper and lower bounds that are close to the actual  $\mu$ -value. As discussed by Lind and Brenner (1999), the computational cost increases with increasing accuracy of the bounds. In practice, for complex valued structured perturbations, relatively tight bounds can be computed in a reasonable time (Young et al., 1991, 1992). For purely real uncertainties, commonly encountered for structural uncertainties, computing accurate bounds can be difficult (Young et al., 1991, 1992; Gu et al., 2012; Heinze and Borglund, 2008).

Several other methods aimed at analysis of how modeling uncertainties affect aeroelastic stability have been proposed. For example, Gu et al. (2012) and Gu and Yang (2012) suggest that the flutter problem, including modeling uncertainties, can be formulated as an optimization problem and that a worst case flutter condition can be solved for by pattern search or by a genetic algorithm. Bueno et al. (2015) suggest a robust analysis method based on linear matrix inequalities and convex optimization. Schwochov (2009) suggests the use of a continuation method in combination with interval modal analysis to investigate how the flutter speed is affected by structural uncertainties. Wu and Livne (2017) use a Monte Carlo based approach to analyze how the aeroelastic stability is affected by aerodynamic as well as structural uncertainties. Marques et al. (2010) apply Monte Carlo, perturbation and interval analysis based propagation methods to analyze how the aeroelastic stability is affected by structural uncertainties while Dwight et al. (2011) apply probabilistic collocation for the same purpose. An overview of methods for uncertainty quantification in aeroelasticity is found in the review by Pettit (2004) as well as in the review by Beran et al. (2017). The review paper by Livne (2003) includes a large number of references related to the subject of uncertainties in aeroelastic analysis.

Relatively recently, the present author (Lokatt, 2014) suggested that perturbations caused by combinations of modeling uncertainties could be analyzed by a method based on eigenvalue differentials (Magnus, 1985) and Minkowski sums (Weibel, 2007). Eigenvalue differentials provide information of how eigenvalues are affected by modeling uncertainties and have previously been used for sensitivity analysis in a wide range of engineering disciplines, as discussed by Li et al. (2014). Also Minkowski sums have found applications in a wide range of subjects, including areas related to reachability analysis (Hagemann, 2015) as well as motion planning, algebraic statistics and decision processes (Weibel, 2010). Based on the information obtained from the eigenvalue differentials, the Minkowski sums allow computation of feasible sets which estimate eigenvalue variations which can be caused by combinations of modeling uncertainties (Lokatt, 2014). For a wide range of uncertainty descriptions, the approach allows an efficient computational procedure making it an interesting alternative for perturbation analysis of systems which are subjected to a large number of structural and aerodynamic uncertainties.

The work presented in this paper concerns the extension of the previously presented perturbation analysis method (Lokatt, 2014) to allow a more general formulation of the structural and aerodynamic system models. The previously proposed method (Lokatt, 2014) requires that the aerodynamic model can be expressed as a function of the polar radius (i.e.  $\mathbf{Q}(p) \approx \mathbf{Q}(r)$  with  $\mathbf{Q}$  being the aerodynamic system matrix,  $p = re^{i\theta}$  the Laplace variable and  $r, \theta$  the polar radius and polar angle respectively) and does not provide a straightforward way of accounting for structural damping, limiting

its usefulness for more general structural and aerodynamic models. In addition, the previous formulation (Lokatt, 2014) is singular at the origin ( $p = 0$ ), complicating the analysis of low frequency instabilities.

In the present work a piece-wise rational polynomial approximation of the aerodynamic model is presented, allowing the flutter equation to be posed as a piece-wise linear eigenproblem. Piece-wise linear eigensystem formulations have previously been proposed by Goodman (2001) and Eller (2009) and, as discussed by Eller (2009), allow a relatively simple solution procedure. The aerodynamic formulation is similar to the rational function approximations (RFA) traditionally employed to find finite-state approximations of the aerodynamic forces (Tewari, 2015) and is easily applicable to aerodynamic data that is pre-computed at a set of reduced frequencies and Mach numbers. A general linear formulation for the structural model is allowed, enabling the inclusion of a model for structural damping, and any type of uncertainty (both structural and aerodynamic) that can be represented by a linear combination of uncertainty matrices can be included in the system formulation. As for the previous method (Lokatt, 2014), the perturbation analysis is based on the computation of eigenvalue differentials (Magnus, 1985) and Minkowski sums (Weibel, 2007).

The presently proposed method combines the computational efficiency of the previously presented perturbation analysis method (Lokatt, 2014) with a general linear system formulation. Since the method allows analysis of how the combined effect of a wide range of structural as well as aerodynamic uncertainties affect the stability of aeroelastic systems, it can provide information which is believed to be helpful for the development of aircraft designs which are more robust with respect to aeroelastic stability.

## 2. Nominal flutter analysis

A nominal system model is found from the flutter equation (Borglund, 2004)

$$[p^2 \mathbf{M} + (b/u)p\mathbf{C} + (b/u)^2 \mathbf{K} - (1/2)\rho b^2 \mathbf{Q}(p)]\mathbf{v} = \mathbf{0}, \quad (1)$$

where  $u$  denotes the airspeed,  $b$  represents an aerodynamic reference length and  $\rho$  denotes the density of the air. Further,  $p = g + ik$  represents the non-dimensional Laplace variable, with  $g$  and  $k$  denoting its real and imaginary parts and  $k$ , also, being the reduced frequency. The mass, damping, stiffness and aerodynamic matrices are denoted by  $\mathbf{M}$ ,  $\mathbf{C}$ ,  $\mathbf{K}$ ,  $\mathbf{Q}$  respectively while  $\mathbf{v}$  represents a displacement vector.

The flutter equation (1), defined in the Laplace domain, forms a non-linear eigenproblem of the eigenvalue  $p$  (Borglund and Eller, 2013), the non-linearity originating from the  $p^2$  term multiplying the mass matrix and the aerodynamic matrix typically being dependent of  $p$  in a non-linear manner. The flutter speed is defined as the lowest speed for which the equation has an eigenvalue  $p$  with positive real part. At this speed, structural deformations corresponding to the flutter eigenvector  $\mathbf{v}$  are sustained and the system is regarded to be unstable. At speeds below the flutter speed (subcritical speeds) structural deformations are damped out and the system is concluded to be stable (Borglund and Eller, 2013).

### 2.1. Aerodynamic model

To allow the flutter equation (1) to be formulated as a set of linear eigenproblems, the complex plane  $P$  is divided into a number of intervals  $P_m$  consisting of points  $p = g + ik$  fulfilling  $k_l \leq k \leq k_u$  where  $k_l$ ,  $k_u$  denote lower and upper bounds of the reduced frequency in the respective intervals. In each interval, the aerodynamic matrix is approximated by a rational polynomial

$$\mathbf{Q}_m(p) = \frac{1}{p} \mathbf{Q}_{-1m} + \mathbf{Q}_{0m} + p \mathbf{Q}_{1m}. \quad (2)$$

To avoid a singular aerodynamic model at the origin, where  $p = 0$ , the linear approximation

$$\mathbf{Q}_m(p) = \mathbf{Q}_{0m} + p \mathbf{Q}_{1m} \quad (3)$$

is used in the interval closest to the origin. The matrices  $\mathbf{Q}_{jm}$ ,  $j = -1, 0, 1$ , are chosen so that the respective element functions  $q_m(p)$  are continuous and continuously differentiable along the imaginary axis. Thus, for all elements  $q(p) \in \mathbf{Q}(p)$ , the linear system

$$q_{0m} + ik_l q_{1m} = q(ik_l) \quad (4)$$

$$q_{0m} + ik_u q_{1m} = q(ik_u) \quad (5)$$

is solved in the first interval whereas the system

$$\frac{1}{ik_l} q_{-1m} + q_{0m} + ik_l q_{1m} = q(ik_l) \quad (6)$$

$$\frac{1}{ik_u} q_{-1m} + q_{0m} + ik_u q_{1m} = q(ik_u) \quad (7)$$

$$\frac{-1}{(ik_l)^2} q_{-1m} + q_{1m} = \left. \frac{dq}{dp} \right|_{p=ik_l} \quad (8)$$

is solved in the following intervals. In the above equations  $i$  denotes the imaginary unit  $\sqrt{-1}$ ,  $q(p)$  denotes an element in  $\mathbf{Q}(p)$  and  $q_{-1m}, q_{0m}, q_{1m}$  denotes the corresponding elements in  $\mathbf{Q}_{-1m}, \mathbf{Q}_{0m}, \mathbf{Q}_{1m}$ . If the aerodynamic matrices have been pre-computed at a set of reduced frequencies  $k_1, k_2, \dots, k_n$ , these values are suitably chosen as boundaries of the intervals  $P_m$  since such a choice ensures that the values of the aerodynamic matrix match the pre-computed values at the specified values of the reduced frequency.

The aerodynamic matrix may not only depend on the Laplace variable  $p$  but also on the Mach number  $M$ , i.e.  $\mathbf{Q}(p, M)$ . The Mach number dependence can be accounted for by computing the coefficient matrices  $\mathbf{Q}_j$  for a set of Mach numbers and employ a suitable interpolation procedure between the pre-computed values. This allows match-point flutter solutions (Lind, 2002) to be computed. In order to simplify the implementation, a constant Mach number is assumed in the present study.

The rational polynomial function bears resemblance to the RFAs commonly used to find finite space approximations for the aerodynamic model (Tewari, 2015). However, while the coefficients in the RFA are typically chosen to find a rational function which, in a suitable measure, is an optimal approximation of the aerodynamic system model (Tewari, 2015), the coefficients in the present formulation are chosen to find an approximation which is piece-wise continuous along the imaginary axis. As such, the present formulation is perhaps more similar to the piece-wise quadratic formulation suggested by Eller (2009). Similar to the piece-wise quadratic formulation (Eller, 2009), the present aerodynamic model may experience jumps at non-zero values of  $g$  when crossing the frequency boundaries  $k_l, k_u$  in between the different intervals  $P_m$ . As discussed by Eller (2009), this can result in corresponding jumps in the eigenvalue paths. However, for the flutter analysis eigenvalues crossing the imaginary axis are of main interest and the possible jumps at non-zero values of  $g$  should presumably not impose a relevant restriction (Eller, 2009).

The main reason for the choice of aerodynamic model is that it allows the flutter equation to be formulated as a piece-wise linear eigenproblem, as will be discussed in Section 2.2. The reason for choosing a piece-wise rational polynomial instead of a piece-wise quadratic polynomial is related to properties of the resulting matrices in the linear system formulation and will be discussed in Section 2.2.

## 2.2. Linear system formulation

With the rational approximation of the aerodynamic model, the system (1) becomes

$$\left[ p^2 \mathbf{M} + (b/u)p\mathbf{C} + (b/u)^2 \mathbf{K} - (1/2)\rho b^2 \left( \frac{1}{p} \mathbf{Q}_{-1m} + \mathbf{Q}_{0m} + p\mathbf{Q}_{1m} \right) \right] \mathbf{v} = \mathbf{0} \quad (9)$$

in each interval  $P_m$ . Introducing  $\mathbf{x}_1 = \frac{1}{p}\mathbf{v}$ ,  $\mathbf{x}_2 = \mathbf{v}$  and  $\mathbf{x}_3 = p\mathbf{v}$ , the flutter equation (9) is reformulated as

$$\mathbf{A}\mathbf{x} = p\mathbf{B}\mathbf{x}, \quad (10)$$

where

$$\mathbf{A} = \begin{bmatrix} \mathbf{0} & \mathbf{I} \\ c\mathbf{Q}_{0m} - e\mathbf{K} & c\mathbf{Q}_{1m} - f\mathbf{C} \end{bmatrix} \quad (11)$$

$$\mathbf{B} = \begin{bmatrix} \mathbf{I} & \mathbf{0} \\ \mathbf{0} & \mathbf{M} \end{bmatrix} \quad (12)$$

in the interval closest to the origin and

$$\mathbf{A} = \begin{bmatrix} \mathbf{0} & \mathbf{I} & \mathbf{0} \\ \mathbf{0} & \mathbf{0} & \mathbf{I} \\ c\mathbf{Q}_{-1m} & c\mathbf{Q}_{0m} - e\mathbf{K} & c\mathbf{Q}_{1m} - f\mathbf{C} \end{bmatrix} \quad (13)$$

$$\mathbf{B} = \begin{bmatrix} \mathbf{I} & \mathbf{0} & \mathbf{0} \\ \mathbf{0} & \mathbf{I} & \mathbf{0} \\ \mathbf{0} & \mathbf{0} & \mathbf{M} \end{bmatrix} \quad (14)$$

in the following intervals. In the above equations the following definitions are employed  $c = (1/2)\rho b^2$ ,  $e = (b/u)^2$ ,  $f = b/u$  and  $\mathbf{x} = (\mathbf{x}_1^T \mathbf{x}_2^T \mathbf{x}_3^T)^T$ .

The system (10) forms a generalized linear eigenproblem. If using a modal basis for the system formulation (Borglund and Eller, 2013), as is common in aeroelastic applications, the mass matrix  $\mathbf{M}$  equals the identity matrix and the system (10) is reduced to an ordinary linear eigenproblem. However, note that the use of a modal basis is not a requirement as the present analysis method is equally well applicable to the generalized eigensystem formulation.

If using a piece-wise quadratic approximation of the aerodynamic model the left hand side matrix in the corresponding linear system (10) would include the  $\mathbf{Q}_{2m}$  matrix (multiplying the  $p^2$  term in the corresponding quadratic aerodynamic approximation  $\mathbf{Q}_m(p) = \mathbf{Q}_{0m} + p\mathbf{Q}_{1m} + p^2\mathbf{Q}_{2m}$ ). While  $\mathbf{M}$  is commonly positive definite (Borglund and Eller, 2013), and thus non-singular, the properties of the  $\mathbf{Q}_{2m}$  matrix are typically unknown. Including  $\mathbf{Q}_{2m}$  in the left hand side matrix could cause it to be singular and, as a result, the linear system could have infinite eigenvalues (Moler and Stewart, 1971). This

could cause difficulties for the flutter analysis. In order to avoid infinite eigenvalues, the left hand side matrix should be non-singular (Moler and Stewart, 1971). With a non-singular  $\mathbf{M}$ , such a matrix is obtained with a rational polynomial approximation of the aerodynamic model and this is the main reason for, in the present study, choosing a rational approximation over a quadratic one.

The system (10) is solved according to the procedure suggested by Eller (2009). A given approximation of the aerodynamic model  $\mathbf{Q}_m(p)$  is assumed to be accurate within the corresponding frequency interval  $P_m$  and thus, eigenvalues fulfilling  $p \in P_m$  are considered to be feasible solutions to (9). Eigenvalues  $p \notin P_m$  are not considered to be feasible solutions to (9), since  $\mathbf{Q}_m$  is not considered to be accurate for  $p \notin P_m$ . The linear eigenproblem (9) is solved for each interval  $P_m$  and the feasible solutions in the different  $P_m$  are assembled to form the total set of feasible solutions to the flutter equation (9).

To find the flutter speed, the system (9) is solved for a set of increasing velocities. If all feasible solutions have negative real part, the speed is considered to be subcritical and the system is concluded to be stable. The flutter speed is reached when some eigenvalue  $p \in P_m$  has a zero or positive real part.

### 3. Perturbation analysis

Introducing mass, damping, stiffness and aerodynamic uncertainties  $d\mathbf{M}$ ,  $d\mathbf{C}$ ,  $d\mathbf{K}$ ,  $d\mathbf{Q}(p)$  to the nominal system matrices the flutter equation (1) becomes

$$[p^2(\mathbf{M} + d\mathbf{M}) + (b/u)p(\mathbf{C} + d\mathbf{C}) + (b/u)^2(\mathbf{K} + d\mathbf{K}) - (1/2)\rho b^2(\mathbf{Q}(p) + d\mathbf{Q}(p))]\mathbf{v} = \mathbf{0}. \quad (15)$$

The corresponding linear system is obtained by replacing the matrices  $\mathbf{M}$ ,  $\mathbf{C}$ ,  $\mathbf{K}$ ,  $\mathbf{Q}(p)$  with  $\mathbf{M} + d\mathbf{M}$ ,  $\mathbf{C} + d\mathbf{C}$ ,  $\mathbf{K} + d\mathbf{K}$ ,  $\mathbf{Q}(p) + d\mathbf{Q}(p)$  respectively in the system matrices (11)–(14). As in previous work (Lokatt, 2014), eigenvalue variations caused by modeling uncertainties are estimated from eigenvalue differentials (Li et al., 2014; Magnus, 1985) and Minkowski sums (Weibel, 2007). The aspects of eigenvalue differentials and Minkowski sums which are of importance for the present work will be discussed in Sections 3.1, 3.2. At this point however, it is sufficient to understand that the uncertainties will cause each eigenvalue to vary within a feasible set, surrounding the nominal eigenvalue, and that an approximation of this set can be found with the above mentioned operators.

To find the solutions of the perturbed flutter equation (15) the complex plane is divided into intervals  $P_m$ . The intervals are chosen in the same way as the frequency intervals in the nominal analysis, as described in Section 2.1. The nominal system eigenvalues  $p_0$  are then computed. For each nominally feasible eigenvalue  $p_0^j$  a feasible set  $S^j$  is computed. Points  $p$  fulfilling  $p \in S^j$  are considered to be feasible solutions to (15) and the feasible solutions in the different  $P_m$  are assembled to form the total set of feasible solutions.

The flutter speed of the perturbed system (15) is found as the lowest speed for which some feasible point  $p$  has a real part larger than, or equal to, zero.

#### 3.1. Eigenvalue differentials

The system formulation (10) allows a general linear uncertainty formulation and thus, any type of structural or aerodynamic uncertainty that can be approximated by a linear combination of uncertainty matrices can be analyzed. Uncertainties  $d\mathbf{K}_i$ ,  $d\mathbf{C}_i$  and  $d\mathbf{Q}_i$  cause variations in the  $\mathbf{A}$  matrix whereas uncertainties  $d\mathbf{M}_i$  cause variations in the  $\mathbf{B}$  matrix. For a given uncertainty, the corresponding eigenvalue differentials are found from Li et al. (2014)

$$p_i^j = \frac{1}{v^{j*} \mathbf{B} u^j} \left( v^{j*} d\mathbf{A}_i u^j - p^j v^{j*} d\mathbf{B}_i u^j \right) \quad (16)$$

where the subscript  $i$  denotes the partial differential with respect to uncertainty  $y_i$  and the superscript  $j$  denotes the index of the eigenvalue, whereas  $v$ ,  $u$  denote the corresponding left and right eigenvectors and the superscript  $*$  denotes the complex conjugate transpose. For the expression (16) to be defined, it is required that

$$v^{j*} \mathbf{B} u^j \neq 0. \quad (17)$$

Assuming  $\mathbf{M}$  to be non-singular (as is commonly the case Borglund and Eller, 2013) the criterion (17) is fulfilled for simple eigenvalues. The case of repeated eigenvalues is discussed by Magnus (1985).

Once the eigenvalue differentials have been computed, a set  $S_i^j$ , within which the eigenvalue  $p^j$  may vary as a result of uncertainty  $i$ , is found from

$$S_i^j = \{\Delta y_i p_i^j \mid \Delta y_i \in I_i\} \quad (18)$$

where  $I_i$  describes a set of feasible values for the uncertainty parameter  $\Delta y_i$ . If  $I_i$  describes a set of real numbers the corresponding eigenvalue variation forms a line in the complex plane whereas if  $I_i$  describes a set of complex numbers (with bounded magnitude and unknown polar angle) the corresponding eigenvalue variation forms a circular area in the complex plane. Structural uncertainties, such as variations in the mass and stiffness matrices, are commonly real valued so that  $I_i$  describes a set of real numbers. Aerodynamic uncertainties may have both unknown magnitude and polar angle, so that  $I_i$  describes a set of complex numbers (Lokatt, 2014).

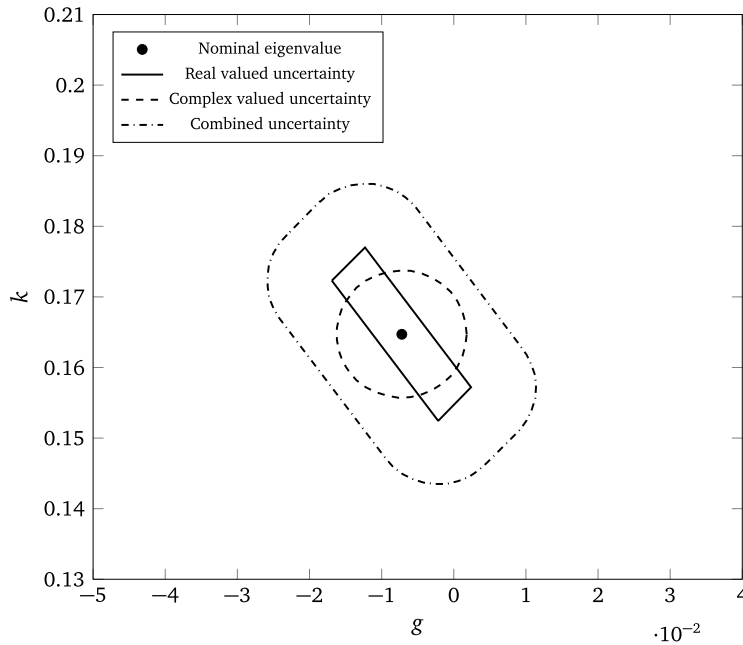


Fig. 1. Illustration of Minkowski sets.

### 3.2. Minkowski sums

In Section 3.1 individual uncertainty sets  $S_i^j$  caused by real valued and complex valued uncertainties were described. In the present section, feasible sets  $S^j$  caused by combinations of individual uncertainties are discussed.

For a set of  $N$  uncertainties, the Minkowski set  $S^j$  surrounding eigenvalue  $p_0^j$  is defined as (Weibel, 2007)

$$S^j = \{p_0^j + p_1^j + p_2^j + \dots + p_N^j \mid p_i \in S_i^j, i = 1, 2, \dots, N\}, \quad (19)$$

i.e. all points which can be written as a linear combination of the linearized eigenvalue perturbations caused by the modeling uncertainties. As such, the set includes all eigenvalue variations which can be caused by the linearized eigenvalue perturbations (16), but does not include any other points, thereby avoiding unnecessarily conservative estimates of the flutter characteristics.

For uncertainty sets in which all individual sets  $S_i^j$  form lines in the complex plane (real valued uncertainties), the feasible set defined by the Minkowski sum is equivalent to a zonotope (Fukuda, 2016), which is a special case of Minkowski sums of polytopes (Weibel, 2007). Combinatorial and computational properties for Minkowski sums of polytopes as well as algorithms for their computation are discussed by Weibel (2007). In the present implementation the Matlab functions *minksum* and *convhull* (The Matlab Works Inc., 1992) are used to find the feasible set. The use of said Matlab functions allows an easy implementation of the proposed perturbation analysis method which is considered suitable for the demonstrative purposes of the present study. While the complexity of the present implementation is unknown, it should be noted that there exist compact and output-polynomial algorithms for the computation of the vertices of a zonotope (Fukuda, 2016) which, presumably, should allow very efficient computation of the feasible sets.

For uncertainty sets in which all individual sets  $S_i^j$  form circular uncertainty areas (complex valued uncertainties), the corresponding Minkowski set is the circular area with radius equal to the sum of the individual uncertainty radii

$$r_a^j = \sum_i r_i^j, \quad (20)$$

where the individual uncertainty radii are found from

$$r_i^j = \Delta y_{i_{\max}} |p_i^j| \quad (21)$$

(this can be seen by considering Euclidian norms for the terms in Eq. (19)). As discussed in previous work (Lokatt, 2014), the evaluation of the feasible sets is in this case particularly simple, as it only consists of computing, and summing, the respective radii (21).

For uncertainty sets which combine linear and circular uncertainty areas (combined real valued and complex valued uncertainties), the Minkowski set is found by computing the zonotope corresponding to the linear uncertainties, and then



extending the feasible set with the uncertainty radius corresponding to complex valued uncertainties (this is found by considering Euclidian norms for the terms in Eq. (19)).

Illustrations of the respective Minkowski sets are shown in Fig. 1. The uncertainty set corresponding to real valued uncertainties illustrates a zonotope. It thus describes the feasible set of eigenvalues which can be reached by adding linearized eigenvalue perturbations corresponding to a set of real valued uncertainties to the nominal system eigenvalue. Similarly, the uncertainty set corresponding to complex valued uncertainties illustrates the circular area which describes the feasible set of eigenvalues which can be reached by adding linearized eigenvalue perturbations corresponding to a set of complex valued uncertainties to the nominal system eigenvalue. The combined uncertainty area illustrates the feasible set which can be reached when considering the combination of both real valued and complex valued uncertainties. As mentioned above, it is found by adding the radius of the circular uncertainty area corresponding to complex valued uncertainties to the feasible set described by the zonotope.

It should be noted that the Minkowski sets provide feasible sets for the *linearized* eigenvalue perturbations found from the eigenvalue differentials, not for the, possibly *non-linear*, eigenvalue variations of the perturbed system model (15). As such, while the Minkowski sum (19) by definition describes a set which encloses all possible eigenvalue variations which are described by the terms in the sum, without adding any extra conservatism, some discrepancy between the predicted eigenvalue sets and the actual eigenvalue variations in the aeroelastic system model can be expected if the actual eigenvalue variations are *non-linear*. The magnitude of the discrepancy depends on the strength of the non-linearity of the eigenvalue variations in the aeroelastic system model. When the perturbations can be considered to be small, the linear estimates are expected to provide relatively accurate estimates of the actual eigenvalue variations and, consequently, the Minkowski sets are expected to provide relatively accurate estimates of the corresponding feasible eigenvalue sets. This will be illustrated in Section 5.

It should be stressed that, since the Minkowski set is a function of the scalar eigenvalue differentials  $p_i^j$ , the complexity of the computation of each Minkowski set depends on the number of uncertainties but, except for the increased cost of computing each  $p_i^j$  which is typically of the order  $m^2$  for a system of size  $m$ , is independent of the size of the nominal system model.

#### 4. Uncertainty description

In order to obtain reliable results from the perturbation analysis it is important to employ an uncertainty model which captures the true variation between the mathematical model and the aircraft dynamics (Borglund, 2003). At the same time, the uncertainty model should not be too large (include parameter perturbations which are highly unlikely to occur), since this can lead to unnecessarily conservative flutter speed estimates (Borglund, 2008; Potter and Lind, 2001). A discussion on different types of uncertainties which may be present in aeroelastic analysis can, for example, be found in the paper by Schwochov (2009) as well as in the review articles by Livne (2003) and Pettit (2004). The present section describes the structural and aerodynamic uncertainty descriptions employed in the present study.

##### 4.1. Structural uncertainty description

In the present work the structural model is posed in a form based on structural eigenvalues and eigenvectors (Borglund and Eller, 2013). With  $n$  basis vectors, the structural stiffness matrix  $\mathbf{K}$  becomes an  $n \times n$  diagonal matrix with diagonal elements  $k_{ii} = (2\pi f_i)^2$ ,  $f_i$  being the  $i$ th structural eigenfrequency.

The uncertainty description is formulated as a variation in structural eigenfrequencies. These are measurable in ground vibration testing (GVT) and, as discussed by Potter and Lind (2001), the GVT results can provide a reference for the magnitude of the modeling uncertainty. Denoting the structural eigenfrequencies of the numerical model by  $f_n$  and the experimentally measured eigenfrequencies by  $f_e$ , the structural uncertainty matrix  $d\mathbf{K}_i$  modeling an uncertainty in eigenfrequency  $i$  is chosen to be a  $n \times n$  diagonal matrix with the  $i$ :th diagonal element equal to  $dk_{ii} = |(2\pi f_{e_i})^2 - (2\pi f_{n_i})^2|$  and all other elements equal to zero. With this uncertainty formulation, elements in the stiffness matrix which are subjected to uncertainties are allowed to be in the range of  $k_{ii} - dk_{ii}$  to  $k_{ii} + dk_{ii}$ . Since only real valued perturbations are considered, the uncertainty description describes real valued uncertainties.

Several authors have used similar uncertainty descriptions, see for example Potter and Lind (2001), Danowsky et al. (2004), Bueno et al. (2015).

##### 4.2. Aerodynamic uncertainty description

Borglund (2004) suggests that the aerodynamic uncertainty can be modeled as a variation in the pressure coefficients in the aerodynamic model. He explains that, for a wide range of aerodynamic models, the aerodynamic matrix can be partitioned into left and right coefficient matrices  $\mathbf{Q}_L$ ,  $\mathbf{Q}_R$

$$\mathbf{Q} = \mathbf{Q}_L \mathbf{Q}_R \quad (22)$$

**Table 1**

Geometry and material information (Doggett and Soistmann, 1989).

Semi span [m]	0.53
Root chord [m]	0.44
Tip chord [m]	0.13
Plate thickness [m]	0.0023
Sweep angle [degrees]	30
Material	Aluminum

**Table 2**

Material properties (Raymer, 1992).

Young's modulus [GPa]	72
Poisson ratio	0.32
Density [kg/m <sup>3</sup> ]	2800

where  $\mathbf{Q}_R$  provides a relation between the structural deformations and the pressure distribution whereas  $\mathbf{Q}_L$  provides a relation between the pressure distribution and the aerodynamic forces. Aerodynamic uncertainty matrices  $d\mathbf{Q}_L$ , modeling the variation in the pressure coefficients are found from

$$d\mathbf{Q}_L = m_a \mathbf{Q}_L d\mathbf{C}_{p_i} \mathbf{Q}_R \quad (23)$$

where  $d\mathbf{C}_{p_i}$  is a diagonal matrix modeling the uncertainty in the pressure coefficients corresponding to uncertainty  $i$  and  $m_a$  denotes the magnitude of the aerodynamic uncertainty (Borglund, 2004). The formulation (23) allows a very detailed uncertainty description since each pressure coefficient can be allowed to vary independently (in both phase and magnitude) of the other pressure coefficients. If there is knowledge about the relation between the pressure variations in different areas of the wing, the information can be incorporated in the uncertainty formulation by including several pressure coefficient uncertainties in one uncertainty matrix (Borglund, 2004).

The uncertainty formulation suggested by Borglund (2008) has shown to be of practical usefulness (Leijonhufvud and Karlsson, 2011) and is the choice of the present work. The aerodynamic uncertainty magnitude is found using an approach similar to  $g$ -validation (Borglund, 2008). That is, the aerodynamic uncertainty magnitude is chosen as the smallest magnitude that explains the difference in damping between an experimentally measured and a numerically computed eigenvalue. As such,  $m_a$  is found from

$$m_a = \frac{|g_e - g_n|}{r_a}, \quad (24)$$

where  $g_e$ ,  $g_n$  denote the real parts of the experimentally measured and the numerically computed eigenvalues whereas  $r_a$  denotes the aerodynamic uncertainty radius found from Eq. (20). The polar angle of the elements in  $d\mathbf{C}_{p_i}$  is considered to be unknown and is assumed to be in the range of 0 to  $2\pi$ . As such, this uncertainty description describes a complex valued uncertainty.

## 5. Model validation

In this section, the above described method is applied to analyze the flutter characteristics of a delta wing model. Flutter predictions provided by the nominal analysis method are compared to experimental results presented by Doggett and Soistmann (1989) as well as to predictions of another numerical method. Variations between the numerical predictions and the experimental results are analyzed by the perturbation analysis method.

### 5.1. Nominal flutter analysis

Geometrical dimensions and material properties of the experimental wing model (Doggett and Soistmann, 1989; Raymer, 1992) are shown in Tables 1 and 2. Based on this data a nominal system model is constructed by creating a structural FEM model and an aerodynamic DLM model in Rodden and Johnson (1994). The FEM model consists of CQUAD4 shell elements with 25 elements in the chordwise direction and 25 elements in the spanwise direction. The DLM model consists of 10 panels in the chordwise direction and 10 panels in the spanwise direction. A modal basis consisting of the eigenvectors corresponding to the ten lowest structural eigenfrequencies is employed. The Nastran model is translated to a format suitable for The Matlab Works Inc. (1992), where the information is used to create a piece-wise linear system as described in Section 2.

A nominal flutter analysis is performed and predicts a flutter speed of 97 m/s and a flutter frequency of 27.6 Hz. For comparison, a flutter analysis is performed using the  $p$ - $k$  solver in Rodden and Johnson (1994). The Nastran analysis predicts a flutter speed of 97 m/s and a flutter frequency of 27.6 Hz, which is equivalent to the predictions of the nominal analysis. A  $v$ - $g$  plot of the system eigenvalues predicted by the nominal analysis method and the  $p$ - $k$  method in Nastran are shown in Fig. 2. It is seen that the eigenvalues computed by both methods are close.



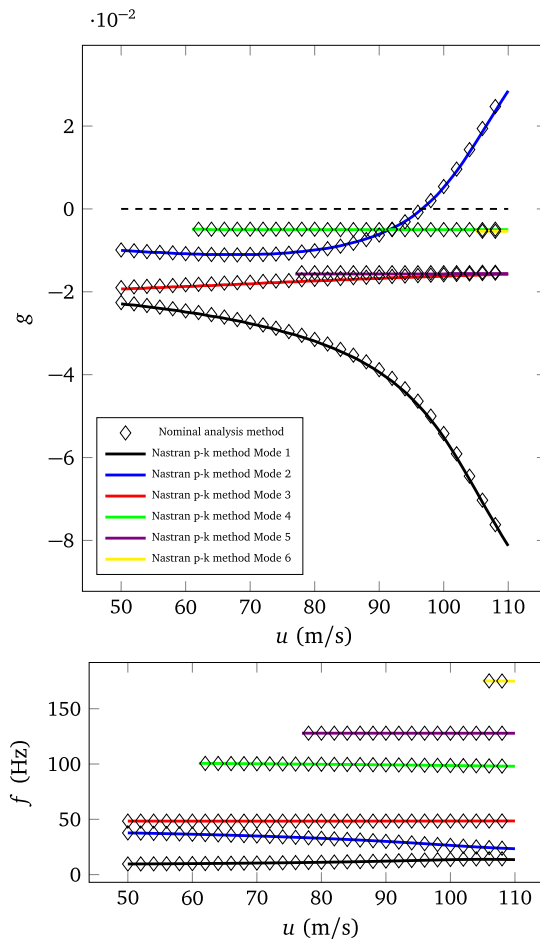


Fig. 2. Nominal flutter solution.

Table 3

Structural eigenfrequencies (Doggett and Soistmann, 1989).

Experimental $f_e$ [Hz]	8.6	38.7	46.8
Numerical $f_n$ [Hz]	9.1	40.3	49.0
Relative variation $\frac{f_n}{f_e}$	1.06	1.04	1.05

The experimental model shows to have a flutter speed of 102 m/s and a flutter frequency of 26.9 Hz. Comparing the numerical predictions to the experimental results it is seen that the nominal analysis under predicts the flutter speed by 6% while the flutter frequency deviates by 1%. In the following section the reason for this deviation is investigated by analyzing uncertainties in the numerical system model.

### 5.2. Uncertainty model

Both structural and aerodynamic uncertainties are considered in the uncertainty formulation. The three lowest structural eigenfrequencies of the experimental model are provided by Doggett and Soistmann (1989) and are shown in Table 3, together with the corresponding frequencies predicted by the numerical model and the relative variation between the experimentally measured and the numerically predicted frequencies. This information is used to find a structural uncertainty description, as described in Section 4.

To find an aerodynamic uncertainty description, the wing is divided into three areas, shown in Fig. 3. The pressure is assumed to vary uniformly within each area (i.e. have the same phase and magnitude) and the uncertainty magnitude is assumed to be the same for all three areas. Since there is little knowledge about the aerodynamic uncertainties, it is unclear whether this is a reasonable assumption. However, the aim of the present test case is mainly to illustrate the usefulness of the perturbation analysis method in accounting for eigenvalue variations caused by parameter perturbations. For this purpose,

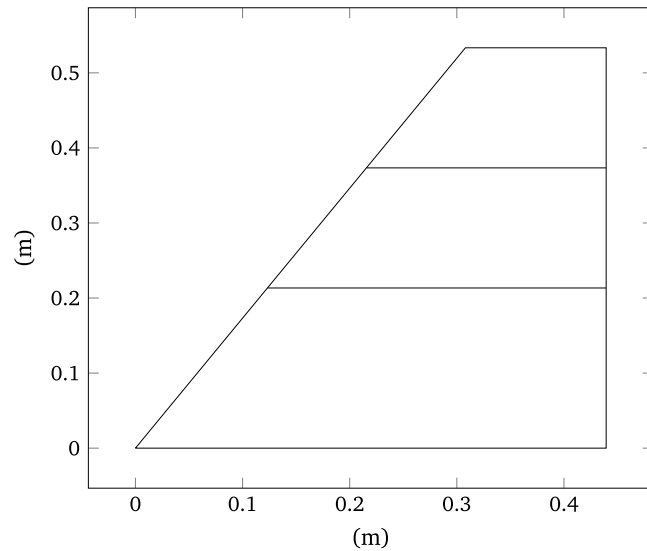


**Fig. 3.** Aerodynamic uncertainty areas.

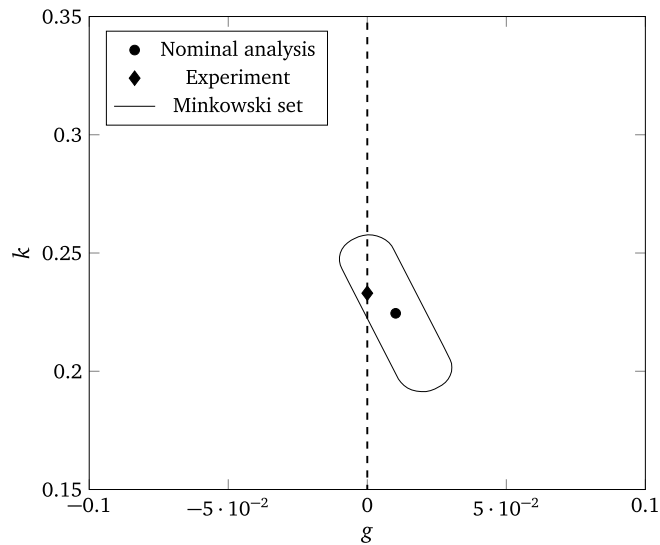


**Fig. 4.** Critical eigenvalue at speed 102 m/s.

it is not necessary that the uncertainty description covers the exact aerodynamic pressure variation, but rather that the uncertainty description is well defined so as to allow comparison to nominal flutter analyses of different combinations of parameter perturbations. For this purpose, the uncertainty description is considered suitable.

The uncertainty magnitude is estimated by evaluating Eq. (24) for the experimental flutter eigenvalue  $p_e = 0.233i$  and the corresponding numerical eigenvalue at the same speed  $p_n = 0.01 + 0.225i$ . This provides an aerodynamic uncertainty magnitude of 0.05, corresponding to 5% of the nominal values of the respective pressure coefficients.

### 5.3. Minkowski sets

Once an uncertainty description has been established, feasible eigenvalue sets are computed according to the procedure described in Section 3. Fig. 4 shows the experimental eigenvalue and the corresponding feasible set predicted by the perturbation analysis method. It is clear that the experimental eigenvalue is a feasible solution to the perturbed eigenvalue system.

However, the perturbation analysis should not only explain the experimental eigenvalue, but predict all possible eigenvalues which could result from parameter variations described by the uncertainty model. To investigate the accuracy

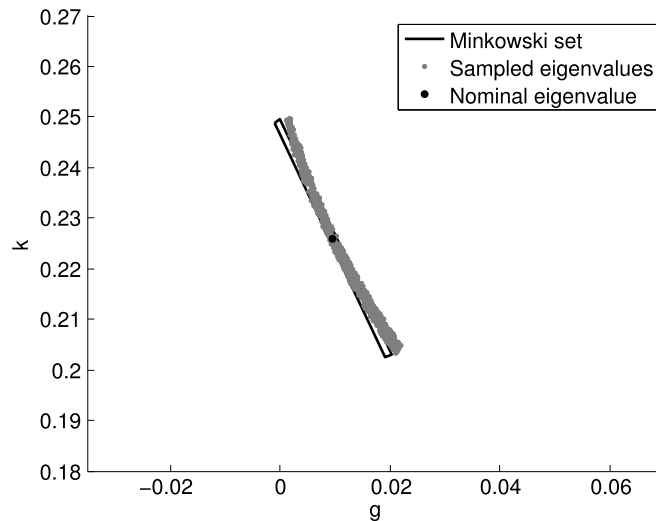


Fig. 5. Critical eigenvalue set for structural uncertainties.

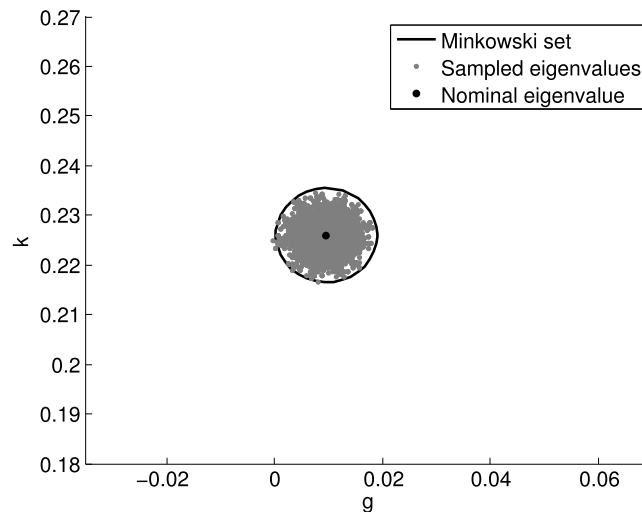


Fig. 6. Critical eigenvalue set for aerodynamic uncertainties.

of the Minkowski sets, the feasible sets predicted by the perturbation analysis method are compared to eigenvalues found from a large number of nominal analyzes.

In a first test only structural uncertainties are considered. The Matlab function *randi* (The Matlab Works Inc., 1992), which samples integer values from a uniform probability distribution function, is used to sample  $10^3$  parameter combinations where each structural uncertainty is allowed to be  $(-1, -0.75, -0.5, -0.25, 0, 0.25, 0.5, 0.75, 1)$  times the maximum uncertainty magnitude. The resulting eigenvalues and Minkowski sets are shown in Fig. 5. While the feasible set predicted by the Minkowski sum has the shape of a polygon, it is seen that the set of eigenvalues obtained from the nominal analyzes has a slightly curved shape. This can be related to the discussion in Section 3.2, as it illustrates that the Minkowski sets provide an uncertainty set based on the linearized eigenvalue differentials which may not be exactly the same as the actual eigenvalue set if the eigenvalue variations are non-linear. Anyhow, it is seen that the Minkowski set provides a relatively accurate approximation of the set of eigenvalues found from the nominal analyzes, as is expected when the uncertainties can be considered to be small.

In a second test, only aerodynamic uncertainties are considered. Each aerodynamic uncertainty is allowed to be  $(0, 0.5, 1)$  times the maximum uncertainty magnitude whereas the phase angle is allowed to be  $(0, \pi/3, 2\pi/3, \pi, 4/3\pi, 5\pi/3)$  radians. A set of  $10^4$  parameter combinations are sampled. The resulting eigenvalues and Minkowski sets are shown in Fig. 6 and it is seen that the feasible set is close to the actual eigenvalue variations.

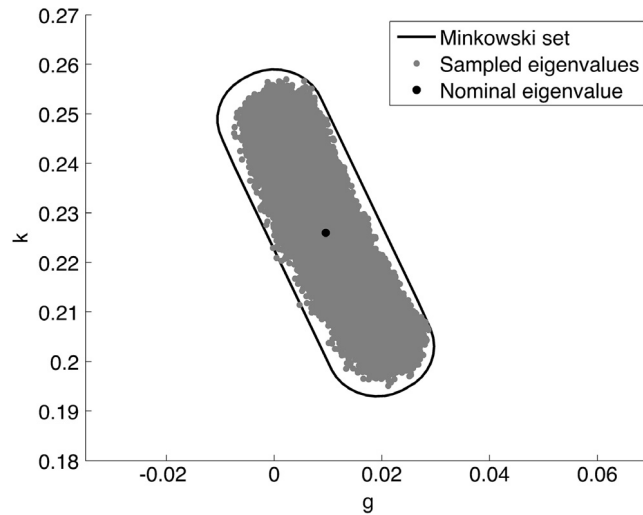


Fig. 7. Critical eigenvalue set for combined structural and aerodynamic uncertainties.

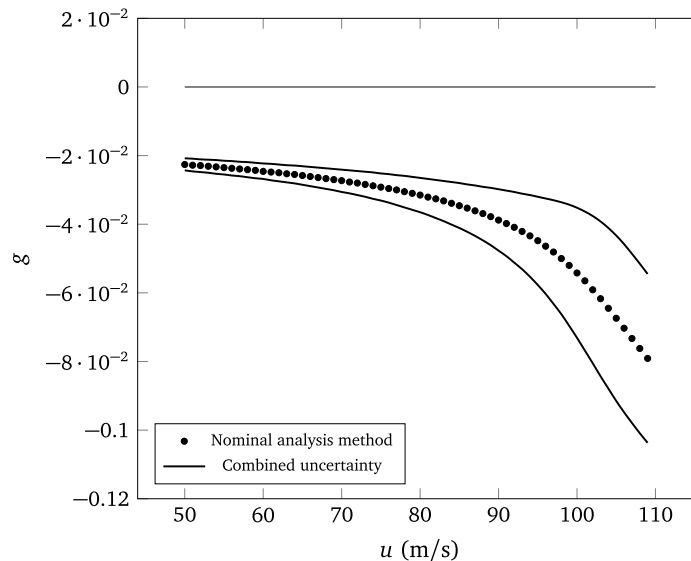


Fig. 8. Damping bounds for Mode 1.

In a third test combined structural and aerodynamic uncertainties are considered. Each structural uncertainty is allowed to be  $(-1, -0.5, 0, 0.5, 1)$  times the maximum uncertainty magnitude whereas the aerodynamic uncertainty parameters are allowed to vary according to the above description. A set of  $10^5$  parameter combinations are sampled. The resulting eigenvalues and Minkowski sets are shown in Fig. 7. It is seen that, again, the feasible set is close to the actual eigenvalue variations.

#### 5.4. Perturbation analysis

Once the accuracy of the Minkowski sets has been established, the perturbation analysis method is applied to compute damping bounds for a set of low frequency eigenmodes. The damping bounds for the critical flutter mode (Mode 2) are shown in Fig. 10. It is seen that the possible variation in damping grows large when the speed is increased. For comparison, the parts of the damping variation caused by the structural uncertainty and the aerodynamic uncertainty respectively are shown in Fig. 11. It is clear that, for this eigenmode, the aerodynamic uncertainty has a larger influence on the damping at subcritical speeds than the structural uncertainty has. However, as the speed increases towards, and above, the flutter speed the structural and aerodynamic uncertainties have a similar influence on the damping. Studying the damping bounds

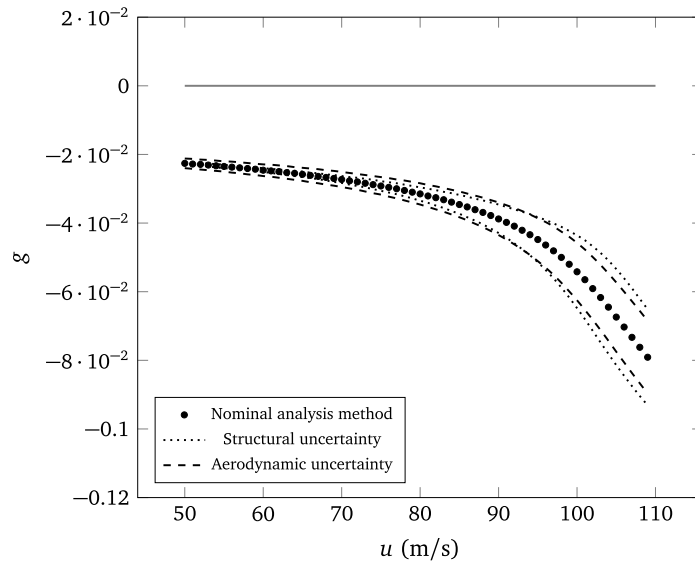


Fig. 9. Damping bounds for Mode 1.

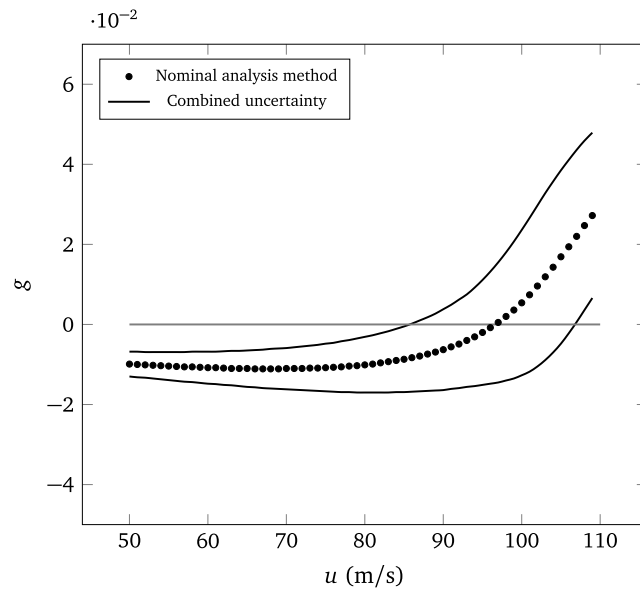


Fig. 10. Damping bounds for Mode 2 (critical flutter mode).

for Mode 1, shown in Figs. 8 and 9, it is found that both the structural and the aerodynamic uncertainties appear to have a relatively small influence on the damping at low speeds, whereas the effect increases for higher speeds. However, the magnitude of the nominal damping for Mode 1 increases with increasing speed and the eigenmode appears to remain stable despite the relatively large variation in damping which could be caused by the modeling uncertainties. Considering the damping bounds for Mode 3, shown in Figs. 12 and 13, the modeling uncertainties appear to have a relatively weak influence on the damping of the eigenmode for all investigated speeds and the eigenmode appears to remain stable.

The results illustrates that both structural and aerodynamic variations can have a considerable effect on the damping of flutter modes. In addition, it shows that modeling uncertainties which do not significantly affect the damping at low subcritical speeds may well be of importance at higher speeds. As such, it highlights the importance of employing an accurate structural and aerodynamic model as well as considering both types of uncertainties in the uncertainty formulation in order to obtain reliable predictions of the flutter characteristics. While the uncertainty formulation employed in the present study

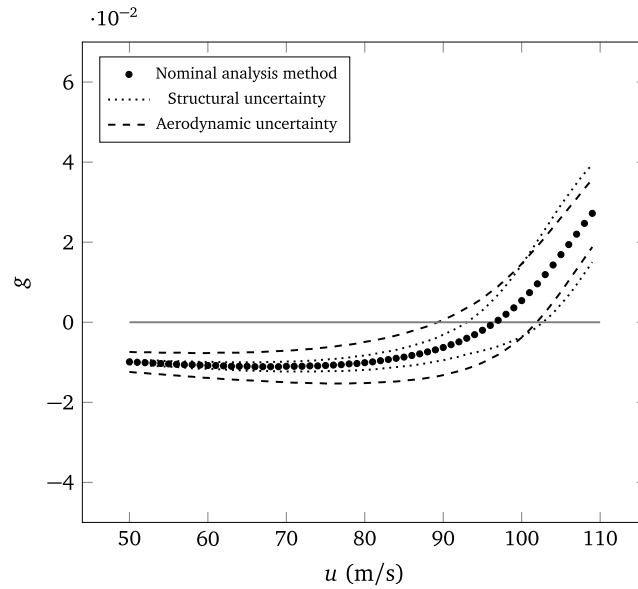


Fig. 11. Damping bounds for Mode 2 (critical flutter mode).

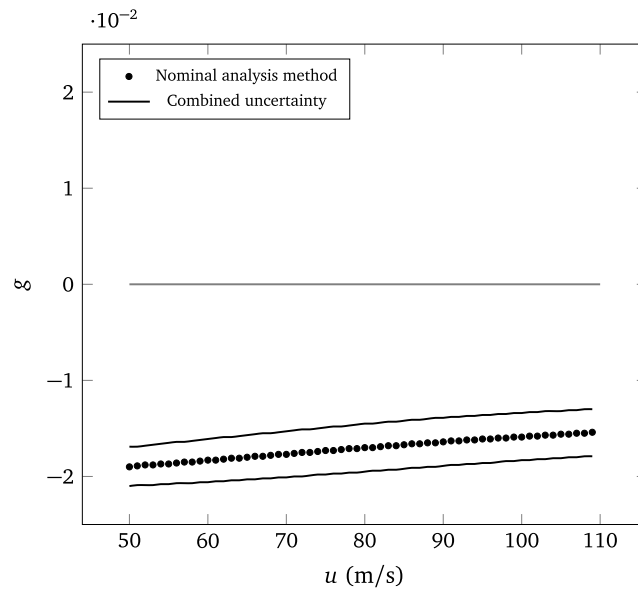


Fig. 12. Damping bounds for Mode 3.

is relatively simple, the general linear system formulation allows a more detailed uncertainty formulation for both structural and aerodynamic uncertainties, which may be beneficial in flutter analysis of more complex aircraft geometries.

## 6. Conclusions

It has been found that both structural and aerodynamic uncertainties can have a notable effect on the damping of the flutter modes and thus need to be considered in order to obtain reliable predictions of the flutter characteristics. As such, the ability to analyze the combined effect of structural and aerodynamic uncertainties is regarded to be a main advantage of the method.

Another considerable advantage of the method is its favorable computational properties, which makes it an attractive option for analysis of systems with a large number of modeling uncertainties.



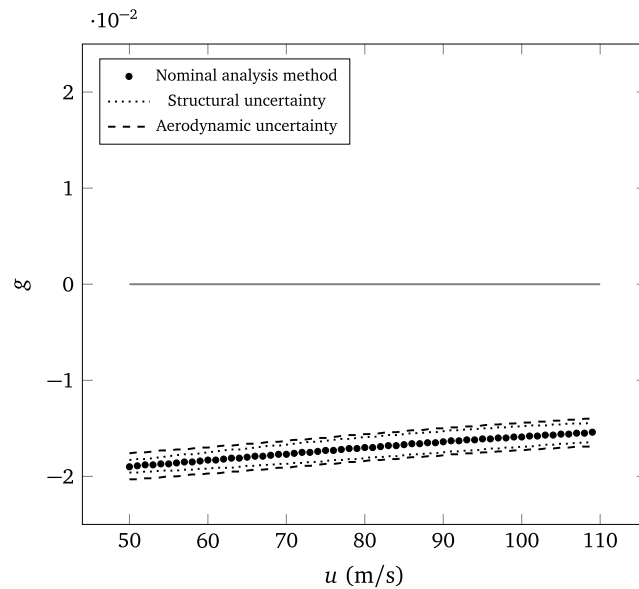


Fig. 13. Damping bounds for Mode 3.

## Acknowledgments

The work presented in this paper was financed partly by the National Aeronautics Research Program (NFFP, Dnr. 2009-01342), coordinated by Martin Leijonhufvud at Saab AB, and partly by the National Aeronautics Research Program (NFFP, Dnr. 2014-00933), coordinated by Roger Larsson at Saab AB. The author would like to thank Ulf Ringertz and Dan Borglund at KTH Royal Institute of Technology for providing scripts which were helpful in extracting the structural and aerodynamic system matrices from Rodden and Johnson (1994) and translating them into a suitable Matlab format (The Matlab Works Inc., 1992). The author would also like to thank David Eller and, again, Ulf Ringertz at KTH Royal Institute of Technology for providing valuable feedback which has been helpful throughout the work.

## References

- Beran, P., Stanford, B., Schrock, C., 2017. Uncertainty quantification in aeroelasticity. *Annu. Rev. Fluid Mech.* 49, 361–386.
- Bisplinghoff, R.L., Ashley, H., 1962. *Principles of Aeroelasticity*. John Wiley and Sons, Inc.
- Borglund, D., 2003. Robust aeroelastic stability analysis considering frequency-domain aerodynamic uncertainty. *J. Aircr.* 40 (1), 189–193.
- Borglund, D., 2004. The  $\mu - k$  method for robust flutter solutions. *J. Aircr.* 41 (5), 1209–1216.
- Borglund, D., 2008. Robust eigenvalue analysis using the structured singular value: The  $\mu - p$  flutter method. *AIAA J.* 46 (11), 2806–2813.
- Borglund, D., Eller, D., 2013. *Aeroelasticity of Slender-Wing Structures in Low-Speed Airflow*. KTH Aeronautical and Vehicle Engineering, Stockholm, Sweden.
- Bueno, D.D., et al., 2015. Flutter analysis including structural uncertainties. *Meccanica* 50, 2093–2101.
- Danowsky, B.P., et al., 2004. Formulation of an aircraft structural uncertainty model for robust flutter predictions. In: 45th AIAA/ASME/ASCE/AHS/ASC Structures, Structural Dynamics & Materials Conference, No. 2004-1853. <http://dx.doi.org/10.2514/6.2004-1853>.
- Danowsky, B.P., et al., 2010. Evaluation of aeroelastic uncertainty analysis methods. *J. Aircr.* 47 (4), 1266–1273.
- Doggett, Jr., R.V., Soistmann, D.L., 1989. *Some Low-Speed Flutter Characteristics of Simple Low-Aspect-Ratio Delta Wing Models*, Tech. Rep. 101547. NASA Technical Memorandum.
- Dowell, E.H., et al., 2015. *A Modern Course in Aeroelasticity*. Kluwer, Dordrecht, The Netherlands.
- Dwight, R., Bijl, H., Marques, S., Badcock, K., 2011. Reducing uncertainty in aeroelastic flutter boundaries using experimental data. In: *International Forum on Aeroelasticity and Structural Dynamics*. IFASD 2011.
- Eller, D., 2009. Flutter equation as a piecewise quadratic eigenvalue problem. *J. Aircr.* 46 (3), 1068–1070.
- Fukuda, K., 2016. Lecture: polyhedral computation, Spring 2016, Department of Mathematics, and Institute of Theoretical Computer Science ETH Zurich, Switzerland, February.
- Goodman, C., 2001. Accurate subcritical damping solution of flutter equation using piecewise aerodynamic function. *J. Aircr.* 38 (4), 755–763.
- Gu, Y., et al., 2012. Robust flutter analysis based on genetic algorithm. *Sci. China* 55 (9), 2474–2481.
- Gu, Y., Yang, Z., 2012. Application of pattern search in worst-case flutter solution. *J. Aircr.* 45 (6), 2089–2092.
- Hagemann, W., 2015. Efficient geometric operations on convex polyhedra, with an application to reachability analysis of hybrid systems. *Math. Comput. Sci.* 9, 283–325.
- Heinze, S., Borglund, D., 2008. Robust flutter analysis considering mode shape variations. *J. Aircr.* 45 (3), 1070–1074.
- Heinze, S., Borglund, D., Ringertz, U., 2009. Assessment of uncertain external store aerodynamics using  $\mu - p$  flutter analysis. *J. Aircr.* 46 (3), 1062–1067.
- Leijonhufvud, M.C., Karlsson, A., 2011. Industrial application of robust aeroelastic analysis. *J. Aircr.* 48 (4), 1179–1183.
- Li, L., et al., 2014. Design sensitivity and hessian matrix of generalized eigenproblems. *Mech. Syst. Signal Process.* 43, 272–294.
- Lind, R., 2002. Match-point solutions for robust flutter analysis. *J. Aircr.* 39 (1), 91–99.

- Lind, R., Brenner, M., 1997. Utilizing flight data to update aeroelastic stability estimates. In: 22nd Atmospheric Flight Mechanics Conference, No. 97-3714, New Orleans, LA, U.S.A.
- Lind, R., Brenner, M., 1999. *Robust Aeroservoelastic Stability Analysis*. Springer, London, Great Britain.
- Lind, R., Brenner, M., 2002. Flight test evaluation of flutter prediction methods, In: 43rd AIAA/ASME/ASCE/AHS/ASC Structures, Structural Dynamics, and Materials Conference, No. 2002-1649, Denver, Colorado, U.S.A.
- Livne, E., 2003. Future of airplane aeroelasticity. *J. Aircr.* 40 (6), 1066–1092.
- Lokatt, M., 2014. A Method for Efficient Flutter Analysis of Systems with Uncertain Modeling Parameters. School of Engineering Sciences, Royal Institute of Technology, Master's thesis.
- Magnus, J.R., 1985. On differentiating eigenvalues and eigenvectors. *Econometric Theory* 1 (2), 179–191.
- Marques, S., Badcock, K.J., Khodaparast, H.H., Mottershead, J.E., 2010. Transonic aeroelastic stability predictions under the influence of structural variability. *J. Aircr.* 47 (4), 1229–1239.
- The Matlab Works Inc., 1992. *MATLAB High Performance Numeric Computation and Visualization Software, Reference Guide*. Prentice-Hall, Inc., New Jersey.
- Moler, C.B., Stewart, G.W., 1971. An Algorithm for the Generalized Matrix Eigenvalue Problem  $Ax = \lambda Bx$ , Tech. Rep. NR 044-377. Center for Numerical Analysis, The University of Texas.
- Pettit, C.L., 2004. Uncertainty quantification in aeroelasticity: Recent results and research challenges. *J. Aircr.* 41 (5), 1217–1229.
- Potter, S., Lind, R., 2001. Developing uncertainty models for robust flutter analysis using ground vibration test data. In: 42nd AIAA/ASME/ASCE/AHS/ASC Structures, Structural Dynamics, and Materials Conference and Exhibit, No. 2001-1585, Seattle, Washington.
- Raymer, D.P., 1992. *Aircraft design: a conceptual approach*. AIAA Education Series, Washington D.C.
- Rodden, W.P., Johnson, E.H., 1994. *MSC/NASTRAN Aeroelastic Analysis Users Guide – Version 68*. The MacNeal-Schwendler Corp., Los Angeles, California.
- Schwochov, J., 2009. Robust flutter analysis using interval modal analysis and continuation method. In: *International Forum on Aeroelasticity and Structural Dynamics*. IFASD 2009.
- Tewari, A., 2015. *Aeroservoelasticity Modeling and Control*. Springer, New York, Heidelberg, Dordrecht, London.
- Weibel, C., 2007. *Minkowski Sums of Polytopes: Combinatorics and Computation*. École Polytechnique Fédérale de Lausanne, Ph.D. thesis.
- Weibel, C., 2010. Implementation and parallelization of a reverse-search algorithm for minkowski sums. In: 2010 Proceedings of the Twelfth Workshop on Algorithm Engineering and Experiments (ALENEX), Austin, Texas.
- Wu, S., Livne, E., 2017. Uncertainty analysis of flutter predictions with focus on the AGARD 445.6 Wing. In: 58th AIAA/ASCE/AHS/ASC Structures, Structural Dynamics, and Materials Conference, Grapevine, Texas.
- Young, P.M., 1991.  $\mu$  analysis with real parametric uncertainty. In: *Proceedings of the 30th Conference on Decision and Control*, Brighton, England.
- Young, P.M., 1992. Practical computation of the mixed  $\mu$  problem, no: 1992 ACC/TM14.